IEEE Photonics Journal
An IEEE Photonics Society Publication



# Holographic Display System Based on Effective Area Expansion of SLM

Volume 11, Number 6, December 2019

Di Wang
Dan Xiao
Nan-Nan Li
Chao Liu
Qiong-Hua Wang

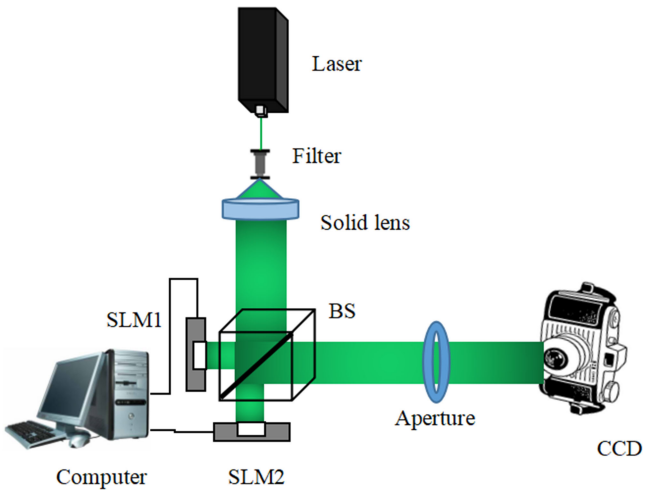


DOI: 10.1109/JPHOT.2019.2947267

# Holographic Display System Based on Effective Area Expansion of SLM

**Di Wang [1,2] Dan Xiao,[3] Nan-Nan Li,[3] Chao Liu,[1,2] and Qiong-Hua Wang [1,2]**

[1]School of Instrumentation and Optoelectronic Engineering, Beihang University, Beijing 100191, China
[2]Beijing Advanced Innovation Center for Big Data-Based Precision Medicine, Beihang University, Beijing 100191, China
[3]School of Electronics and Information Engineering, Sichuan University, Chengdu 610065, China

*DOI:10.1109/JPHOT.2019.2947267*


Manuscript received September 15, 2019; revised October 6, 2019; accepted October 10, 2019. Date of publication October 14, 2019; date of current version October 5, 2019. This work was supported in part by the National Natural Science Foundation of China under Grant 61535007 and in part by the project funded by China Postdoctoral Science Foundation under Grants 2019M650422 and 2019M650421.
Corresponding author: Qiong-Hua Wang (e-mail: qionghua@buaa.edu.cn).

**Abstract:** In this paper, a holographic display system with wide viewing area is proposed based on the effective area expansion of the SLM. The effective area of the SLM is calculated based on the viewing area characteristics and expanded by using two SLMs. Different from the traditional holographic system based on the parallel-arranged SLMs or curved-arranged SLMs, we calculate the effective areas of the SLMs and the effective hologram of the system can be generated based on the effective-viewing-area (EVA) algorithm. The proposed system uses a 4K SLM by seamlessly stitching the effective areas of two 2K SLMs. After the EVA is calculated, the size of the effective hologram is inversely calculated according to the EVA. So, the effective area of the hologram is increased, and the calculation of the wasted information is greatly decreased. With the proposed system, the reconstructed object with large viewing area can be realized. Moreover, the calculation time for generating the hologram is reduced significantly. Experimental results verify the feasibility of the proposed system. In the proposed system, the 2K SLMs are used as examples for splicing, when more high-performance SLMs are used, the viewing area will be further expanded, and the advantage of the calculation speed will be more obvious than the traditional splicing method. The proposed system can provide new references to the holographic display system based on multiple SLMs stitching.

**Index Terms:** Spatial light modulator, holographic display, hologram.

## 1. Introduction

The acquisition and display of three-dimensional (3D) information have always been a hot topic [1], [2]. Recently, researchers hope to develop a true 3D display that can be viewed freely by observers from different angles. As a unique technique, the holographic display can record and reconstruct the wavefront information of the light wave [3]. Therefore, the true 3D object can be reconstructed and there is no conflict between the convergence and accommodation of human eyes. Thus, the holographic display is expected as an ideal way of the 3D display [4], [5]. However, limited by the parameter of the spatial light modulator (SLM), the viewing angle and area of the reconstructed object are extremely small [6]–[9]. In addition, as each point in the hologram records the entire

information of the 3D scene, the computational complexity is so high that it is difficult to achieve real-time generation of the hologram [10], [11].

Various methods and systems have been proposed to solve the problems. Some researchers use the shutters or Galvano mirror to enlarge the viewing area based on the time-division multiplexing [12]–[14]. Besides, a potential method has also been proposed by using the lens array and shutters to upload holograms on the SLM in turns [15]. Although the methods based on time-division multiplexing can solve the problem of the small viewing area, it is impossible to arrange the SLM seamlessly. Thereby, these methods may miss parts of the viewing area. In 2011, the method by reallocating the resolution of the SLM was realized by using a 4f imaging system [16]. The horizontal viewing angle of the SLM can be enlarged by increasing the horizontal resolution of the SLM, while the vertical viewing angle was decreased. Different from the method based on an SLM, the methods based on the space-division multiplexing by using multiple SLMs have also been studied a lot [17], [18]. The original system used multiple SLMs which were arranged in parallel to expand the holographic viewing area [19], [20]. However, the utilization rate of the light energy is relatively low due to the gaps between the SLMs. In 2011, a curved holographic system by splicing twelve SLMs together was proposed [21]. Each tilted SLM was loaded with the hologram which contained the information of a certain viewing angle of the object. The system calculated the hologram information according to the point cloud data, and the resolution of the calculated hologram was equal to the size of the SLM. In 2014, a holographic system with large viewing angle was achieved based on two SLMs [22]. The viewing angle of the reconstructed object can be continuously expanded to 27.5° by using a movable cylindrical lens. In 2016, a holographic display system with increased space bandwidth product was proposed by using diffractive optical elements (DOEs) to form a combined wave field [23]. In 2017, a system by using two SLMs and a 4f concave mirror was built to reconstruct the image with the viewing angle of 12.8° [24]. In 2018, a wide viewing-zone holographic display was proposed by using a convex parabolic mirror [25]. Meanwhile, many calculation algorithms have been proposed in order to realize the holographic display with wide viewing angle. In 2018, a complex amplitude modulation method was proposed for color holographic display with wide viewing angle [26]. Besides, the method of generating 360° color holograms has also been studied [27].

Though the systems to expand the viewing area have been considered, the calculations of the hologram and the viewing area cannot meet the requirement of the real-time display. In order to realize the holographic display with high quality, various algorithm acceleration methods have been proposed, such as look-up table [28], [29], wavefront recording method [30] and compressed look-up table [31], [32]. Nowadays, it is still difficult to achieve fast holographic display with large viewing area. Although there are many problems in the holographic display that need to be solved, the researchers have never stopped the research.

In this paper, a holographic display system with wide viewing area is proposed based on the effective area expansion of the SLM. The corns of the proposed system are two SLMs and a beam splitter (BS). The hologram plane is composed of two SLMs and the two SLMs are seamlessly stitched together as a 4K SLM device. By analyzing the effective area of the 4K SLM, the effective hologram of the system can be generated with the EVA algorithm. In this way, the effective area of the hologram is calculated, and the calculation of the wasted information is decreased compared with the traditional system. With the proposed system, the reconstructed object with large viewing area can be realized. Moreover, the calculation speed is improved.

## 2. Structure and Operating Principle

Fig. 1 shows the structure of the proposed system based on two SLMs. It consists of a laser, a filter, a solid lens, a BS, two SLMs, a computer, an aperture and a CCD. The laser, filter and solid lens are used to generate the uniform parallel beam for irradiating the two SLMs and reconstructing the objects. The BS is located in the emission direction of the parallel beam and divides the beam into two beams which are perpendicular to each other. The two SLMs with the resolution of $1920 \times 1080$

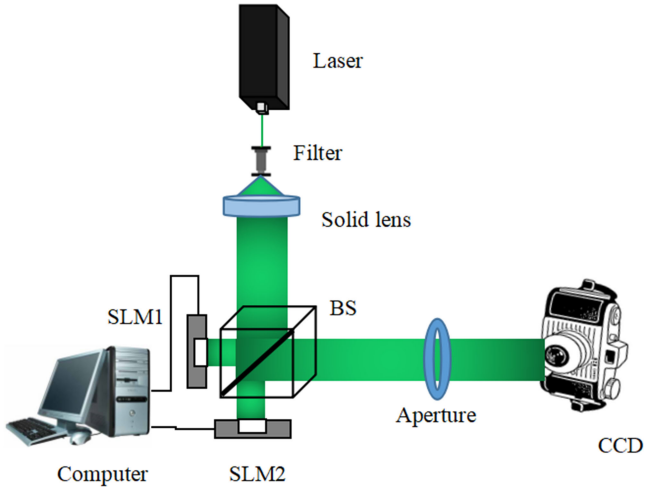


Fig. 1. Structure of the proposed system based on two SLMs.

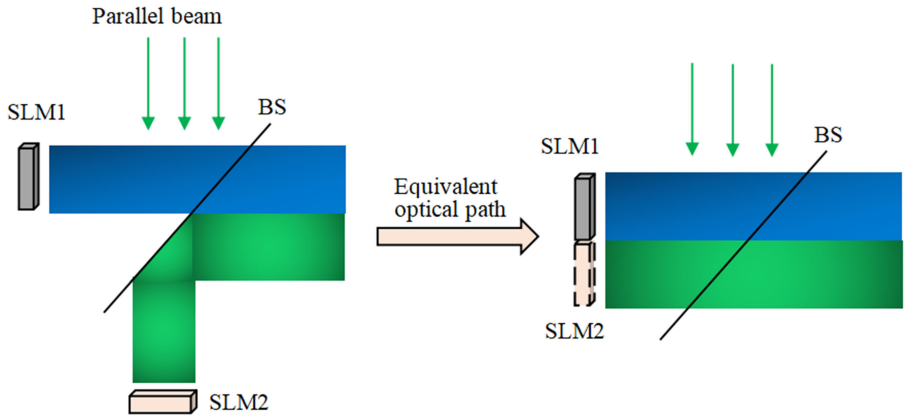


Fig. 2. Composition principle of the 4K SLM.

(2K) are located in the emission direction of two beams respectively. Then the diffraction lights of the two SLMs can pass through the BS and the reconstructed object can be captured by the CCD.

The corns of the proposed system are the SLMs and BS. Equivalently, the two SLMs and a BS can be considered as a SLM with 4K resolution, as shown in Fig. 2. Different from the conventional 4K resolution, the 4K resolution of the proposed system refers to the horizontal direction. When the light passes through the BS, half of the light wave is reflected on SLM1 and the other half illuminates SLM2. The two SLMs are placed orthogonally, and they can be equivalently viewed as two SLMs that are seamlessly stitched together on the same plane. Then we regard the SLMs as a 4K SLM. Fig. 3 shows the geometric relationship between the 4K SLM and the EVA of the reconstructed object. In the holographic reconstruction, when the hologram is loaded on the SLM irradiated by the uniform parallel beam, the amplitude and phase information of the light wave is modulated. The diffraction angle $\alpha$ satisfies the following equation:

$$\alpha \leq \sin^{-1}\left(\frac{\lambda}{2p}\right), \tag{1}$$

where $\lambda$ represents the wavelength of the light and p denotes the pixel size of the 4K SLM. According to the geometric relationship and (1) we know that when the diffraction angle is extremely small,

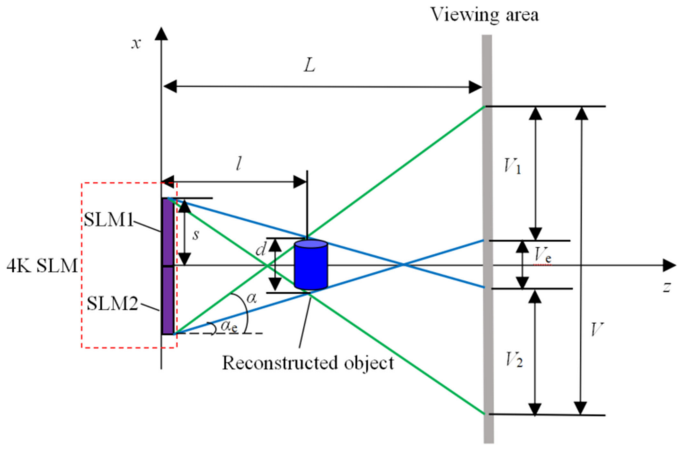


Fig. 3. Geometric relationship between the 4K SLM and the EVA of the reconstructed object.

the size of the reconstructed object d can be expressed as follows:

$$\alpha \approx \sin\alpha \approx \tan\alpha = \frac{h+d}{2l} \leq \frac{\lambda}{2p}, \tag{2}$$

$$d \leq \frac{\lambda l}{p} - h, \tag{3}$$

where l represents the effective propagation distance from the SLM to the reconstructed object, s represents the height of the 2K SLM, and h = 2 s represents the height of the 4K SLM.

In order to analyze the effective viewing area, the maximum viewing angle of the reconstructed object is calculated, which can be expressed as follows:

$$\alpha_e = \frac{2s-d}{2l}, \tag{4}$$

where $\alpha_e$ is the maximum viewing angle of the reconstructed object. The viewing area calculated by the maximum viewing angle is described in blue lines. According to the geometrical relationship, we can see that the maximum viewing angle of the reconstructed object is smaller than $\alpha$. In principle, $V$ represents the whole size of reconstructed object field. However, only in the area $V_e$ the complete reconstructed object can be seen according to the principle of the holographic diffraction. In the areas $V_1$ and $V_2$, only a part of the reconstructed object can be seen. Since we can not see the complete image at $V_1$ and $V_2$, these areas are called wasted areas. When the eyes are placed on the wasted areas, the motion parallax of some 3D images will be seen from this position, but we do not consider it in the proposed system. So, the area $V_e$ is called the EVA of the reconstructed object, which can be expressed as follows:

$$V_e = 2L\tan\alpha_e - 2s, \tag{5}$$

$$V_e = \frac{2s(L-l) - dL}{l}, \tag{6}$$

where $L$ is the distance between the SLM and the viewing area. On the other hand, the size of the waste filed $V_w$ satisfies the following equation:

$$V_w = V_1 + V_2 = \frac{2dL}{l} \leq 2\left(\frac{L\cdot\lambda}{p} - \frac{2L\cdot s}{l}\right). \tag{7}$$

When the object point is reconstructed, two red lines are used to represent the diffracted light boundary, the blue solid lines and green lines are parallel to each other, as shown in Fig. 4. For an object point, if its entire hologram is recorded, the area of the diffraction light is larger than $V_e$ according to the analysis. In the proposed system, we only record the necessary interferogram.

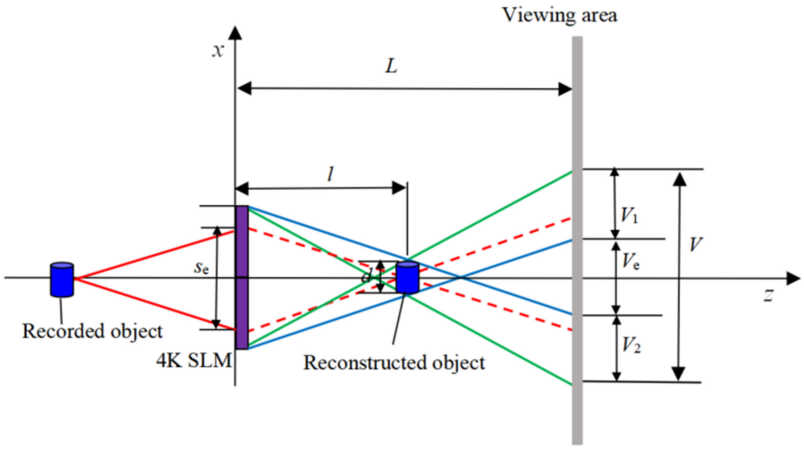


Fig. 4. Relationship between the recorded object, SLM, reconstructed object and the EVA.

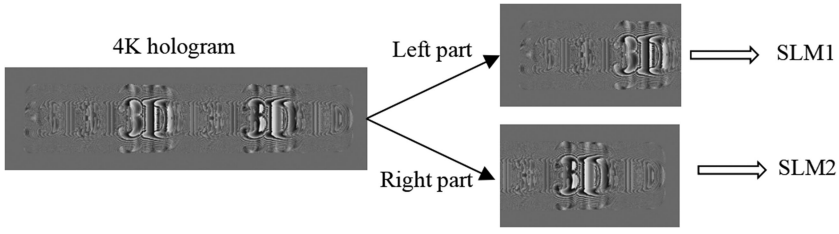


Fig. 5. Processing of the 4K hologram.

According to the geometric relationship, the size of the necessary interferogram $S_e$ satisfies the following equations:

$$S_e = 2s - d, \tag{8}$$

$$re(S_e) = \text{int}\left(\frac{S_e}{p}\right), \tag{9}$$

where int() represents the rounding operation. According to the EVA and geometric analysis of the proposed system, the effective area of the SLM can be calculated, and the size of the effective hologram can be calculated accordingly. As can be seen from (8), the hologram size loaded on the SLM is smaller than the size of the SLM. Moreover, the size of the recorded object needs be smaller than that of the SLM, and the size of the necessary interferogram is equal to the difference between the size of the SLM and the recorded object. In the process of the hologram generation, the resolution of the effective hologram is not 4K. Based on the EVA analysis, we generate a hologram based on the necessary interferogram. The necessary interferogram is generated according to the scalar diffraction principle and the viewing zone characteristics of the reconstructed object. Then the interferograms of other points on the same depth of the recorded object are obtained by translation of the necessary interferogram. In the proposed system, the novel-look-up-table (NLUT) algorithm improved by the EVA method is used to generate the hologram [33]. The principal fringe pattern (PFP) is pre-calculated and the resolution of the PFP is smaller than that of the SLM according to the EVA calculation. The effective hologram pattern can be generated by using shifting and adding operations of PFP based on the property of shift invariance. To match the resolution of the SLM, the hologram is surrounded by a grayscale image filled with zero. The effective hologram is loaded on the effective area of the 4K SLM, as shown in Fig. 5. The final 4K hologram is divided equally into two parts, and the holograms of the left and right parts are loaded onto the two 2K SLMs,

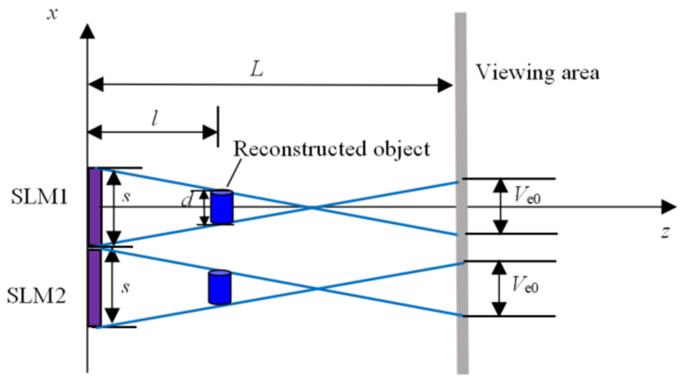


Fig. 6. EVA analysis of the traditional system.

respectively. When the light illuminates the 4K SLM, we can see the reconstructed object at the viewing area.

In the proposed system, two 2K SLMs are regarded as a 4K SLM. Then we analyze the traditional system in which two SLMs are placed in parallel and not regarded as a 4K SLM, as shown in Fig. 6. We use traditional algorithm to generate the 2K hologram of the recorded objects and load the same hologram on two SLMs. When the holograms of the recorded object are loaded on two SLMs, the effective viewing area for each SLM can be analyzed according to the diffraction theory. According to the above analysis, we know that for an SLM, the EVA satisfies the following equation:

$$V_{e0} = \frac{s(L - l) - dL}{l}, \tag{10}$$

where $V_{e0}$ is the EVA of a single SLM. The EVA of the traditional system in which two SLMs are placed in parallel is $2V_{e0}$ and it can be expressed as follows:

$$2V_{e0} = \frac{2s(L - l) - 2dL}{l} < V_e, \tag{11}$$

As can be seen from Fig. 6, there are some intervals between the two EVAs, in which the complete reconstructed image cannot be seen. Then the EVA of such a system is discontinuous. The traditional systems which splice multiple SLMs just like Fig. 6 only consider the viewing area expansion of the reconstructed image, but do not consider the continuous viewing and expansion of the EVA. So, we can see that by using the proposed system, the EVA can be expanded. Moreover, the calculation speed is improved since the wasted field is reduced by using our proposed system. As the size of the recorded object increases, the increase in the reproduced EVA is more pronounced. Besides, there are some system that treat two SLMs as a 4K SLM. In the calculation process, a 4K hologram of the recorded object is generated directly and evenly divided into two parts to be loaded on two SLMs. Although the viewing area can also be expanded, the wasted viewing area is not needed and the calculation of the wasted information will affect the calculation speed.

## 3. Experiment and Discussion

In order to demonstrate the feasibility of the proposed system, we conducted the experiments. A green laser, a filter, a solid lens, two SLMs, a BS, an aperture and a CCD are used in the experiment. The green laser with the wavelength of 532 nm is used as the light source. The focal length of the solid lens is 300 mm. The BS has the size of 25.4 mm $\times$ 25.4 mm and the transmission rate of 80%. The models of the two SLMs are the same (the pixel pitch is 6.4 $\mu$m; the pixel number is 1920 $\times$ 1080; the size of the SLM panel is 12.29 mm $\times$ 6.91 mm). The 4K SLM has the pixel number of 3840 $\times$ 1080. Firstly, we conduct a basic experiment with a single SLM. The letter 'H'

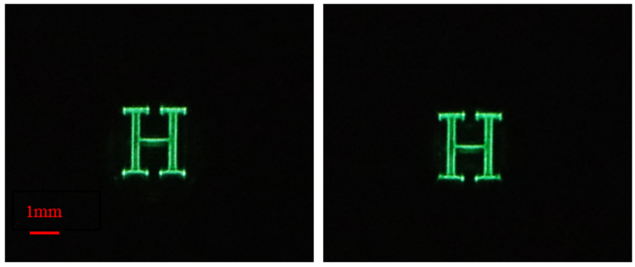


Fig. 7. Reconstructed object with a single SLM. (a) Reconstructed object by using the traditional NLUT method. (b) Reconstructed object by using the EVA calculation.

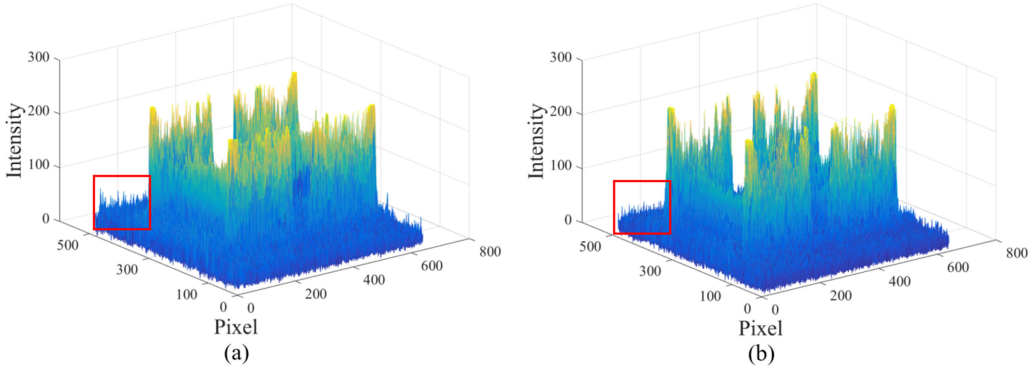


Fig. 8. Intensities of the reconstructed object. (a) Intensity of Fig. 7(a). (b) Intensity of Fig. 7(b).

with the resolution of 320 × 240 is used as the recorded object. The SLM1 is turned on and the SLM2 is turned off at the same time. The hologram with the resolution of 1920 × 1080 is generated by using the traditional NLUT method and the reconstructed object is shown in Fig. 7(a). When the EVA calculation method is used to generate the hologram, the resolution of the effective hologram is 1600 × 840 and the reconstructed object is shown in Fig. 7(b). As can be seen from the results, the reconstructed object by using the EVA calculation can be displayed with a good quality. At the same time, the calculation speed by using the EVA calculation can be improved since the wasted information is reduced. The intensities of the reconstructed objects are shown in Fig. 8, where Fig. 8(a) and Fig. 8(b) are the intensities of Fig. 7(a) and Fig. 7(b), respectively. From the red box we can see that the speckle noise of the EVA calculation is better than that of the traditional NLUT method. The average point calculation time by using the traditional NLUT method and the EVA calculation is ∼0.024 s and ∼0.017 s, respectively. Through simulation, the peak signal to noise ratio (PSNR) values of the traditional method and our method are ∼28 and ∼35, respectively.

Then the 4K SLM is used for the experiment. When the light is used to illuminate the SLM, the zero-order light can be detected by the CCD. Fig. 9(a) is the zero-order light of the single SLM, and Fig. 9(b) is zero-order light of the 4K SLM. It can be seen clearly that the zero-order light can be seamlessly spliced together. In order to verify the versatility of the proposed system, the simulation experiment has been conducted. The letter 'W' and a car are used as the recorded objects. The resolution of the recorded objects is 960 × 720. Then the PFP is pre-calculated and the resolution of the PFP is 2880 × 1080. So, the effective hologram of the recorded object can be calculated, and the resolution of the effective hologram is 2880 × 1080. Then the effective hologram is loaded on the effective area of the 4K SLM, that is, both SLM1 and SLM2 are loaded on the effective hologram with the resolution of 1440 × 1080.

Fig. 10 is the simulation result of the reconstructed object, where Fig. 10(a) is the result by using the 4K SLM and Fig. 10(b) is the result by using a single 2K SLM. The average point calculation

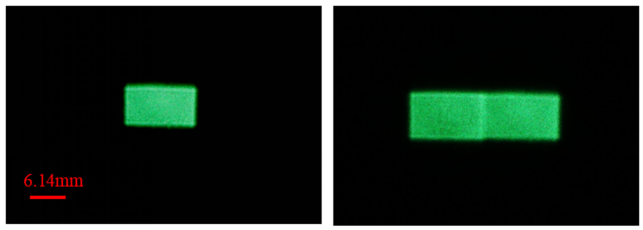


Fig. 9. Zero-order diffraction light. (a) Zero-order diffraction light of a single SLM. (b) Zero-order diffraction light of the 4K SLM.

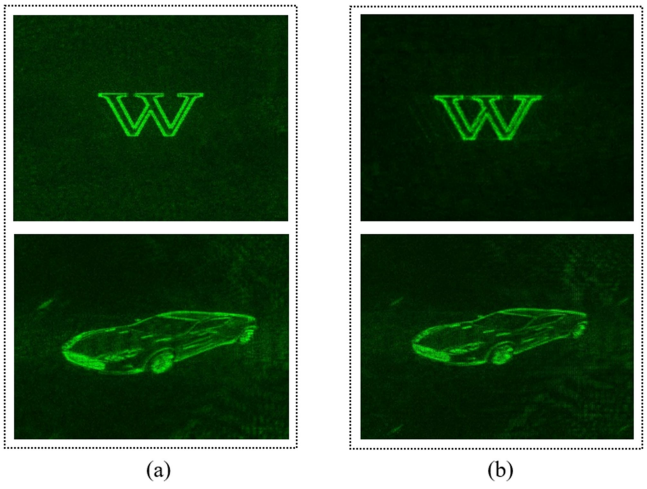


Fig. 10. Simulation results of the reconstructed object. (a) Reconstructed object by using the 4K SLM. (b) Reconstructed object by using the 2K SLM.

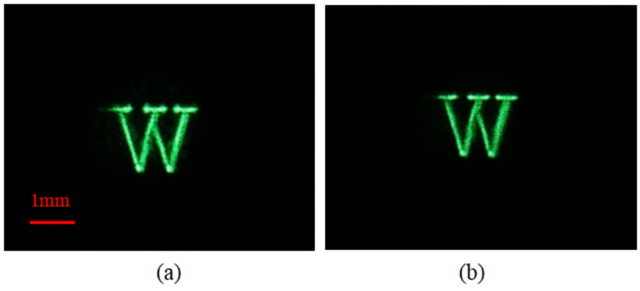


Fig. 11. Optical experiment result. (a) Result of the reconstructed object by using the proposed system. (b) Result of the reconstructed object by using the traditional holographic system.

time of 'W' in Fig. 10(a) and Fig. 10(b) is ∼0.036 s and ∼0.024 s, respectively. However, the average point calculation time by using the system in Fig. 6 is ∼0.049 s. The simulation results show that the intensities by using the proposed system is higher than that by using the 2K SLM. Besides, experiment has been conducted in order to analyze the advantages of the proposed system compared with the traditional system based on parallel-arranged SLMs.

The optical experiment result is shown in Fig. 11. In the experiments, when the light is used to illuminate the 4K SLM, the object can be reconstructed with a larger viewing area. The width of the viewing area is also analyzed, as shown in Fig. 12. Fig. 12(a) and Fig. 12(b) record the light

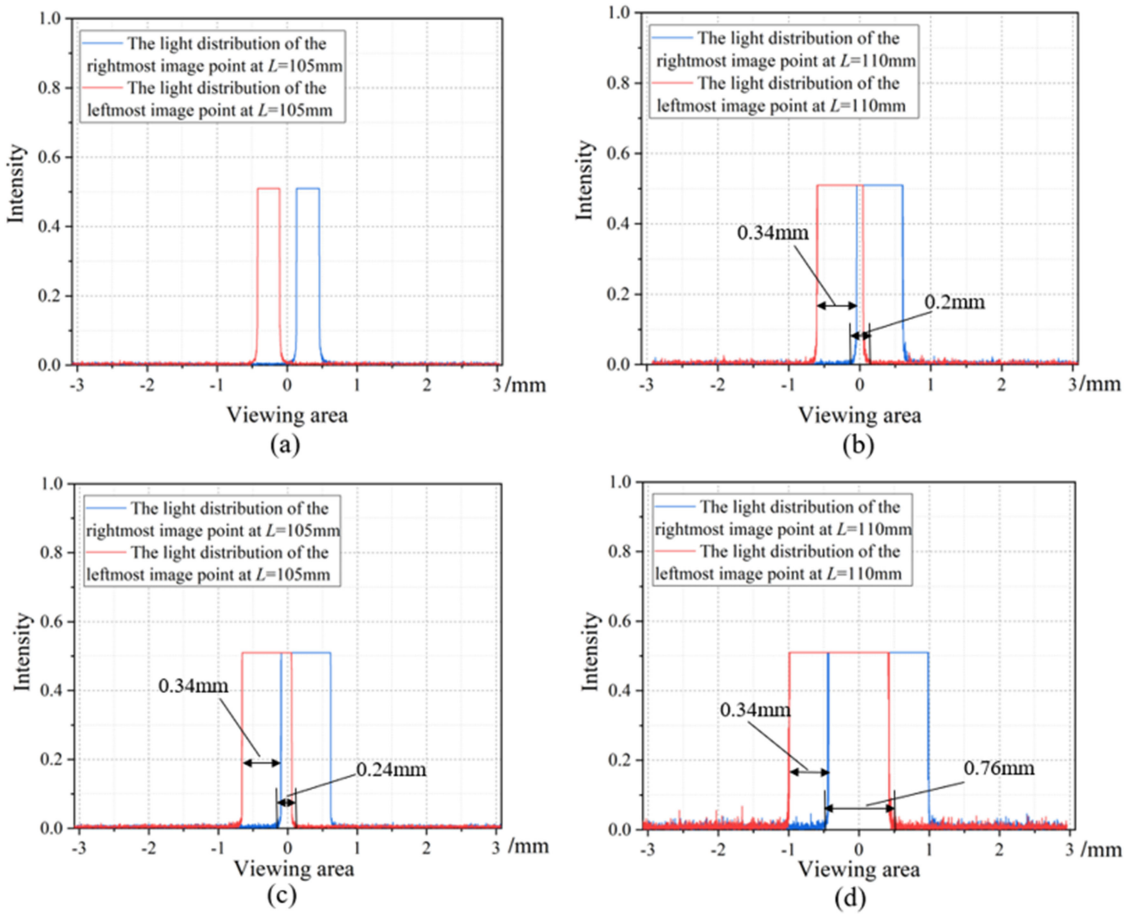


Fig. 12. Light distribution of the image points. (a) Light distribution of the leftmost and the rightmost image points by using the traditional 2K SLM system at L = 105 mm. (b) Light distribution of the leftmost and the rightmost image points by using the traditional 2K SLM system at L = 110 mm. (c) Light distribution of the leftmost and the rightmost image points by using the proposed system at L = 105 mm. (d) Light distribution of the leftmost and the rightmost image points by using the proposed system at L = 110 mm.

distribution of the leftmost and the rightmost image points by using the traditional 2K SLM system at $L = 105$ mm and $L = 110$ mm, respectively. Fig. 12(c) and Fig. 12(d) are the light distribution of the leftmost and the rightmost image points by using the proposed system at $L = 105$ mm and $L = 110$ mm. It can be seen clearly that the proposed system has a larger viewing area. Compared with the traditional 2K SLM system, the EVA of the proposed system is increased. When two SLMs are placed in parallel by using the traditional system such as Fig. 6, the EVA can be calculated according to Eqs. (10)–(11). It is easy to conclude that the EVA of the traditional system based on parallel-arranged is smaller than that of the proposed system. Moreover, according to Eq. (11) we know that when L and d changes, the difference of the EVAs between the proposed system and the traditional system changes accordingly. So, when the distance of the viewing area is increased, the proposed system will have a larger viewing area, as shown in Fig. 12(d).

Compared with the conventional method based on a single 2K SLM, the width of the EVA based on proposed system is increased by ∼280%. Therefore, this experiment proves that the proposed system significantly enlarges the EVA of the reconstructed objects. Compared with the traditional system in Fig. 6 where two SLMs are arranged in parallel, the width of the EVA based on the proposed system is increased by ∼90%. At the same time, the calculation speed of the proposed system is analyzed, as shown in Fig. 13. From Fig. 13 we can

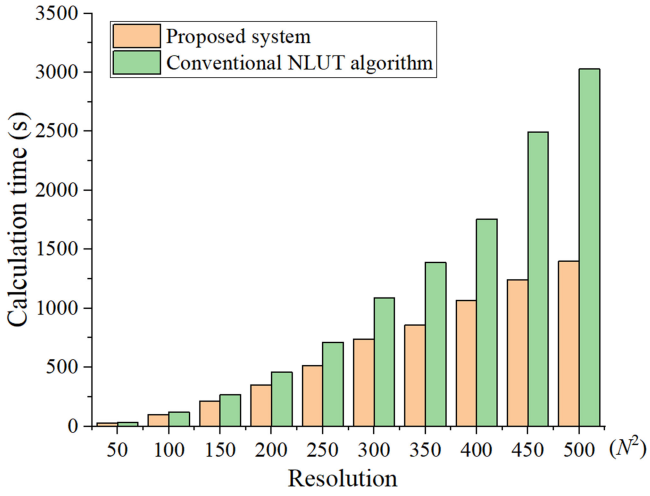


Fig. 13. Relationship between the calculation time and the resolution of the recorded object.

see that the calculation time increases accordingly when the resolution of the recorded object increases.

In the proposed system, the calculation method for generating the hologram is different. Different from the traditional system, the proposed system adopts the EVA algorithm. According to the EVA and geometric analysis of the proposed system, the effective area of SLM can be calculated, and the size of the effective hologram can be calculated accordingly. As can be seen from (8), the hologram size loaded on the SLM is smaller than the SLM size. The size of the necessary interferogram is equal to the difference between the size of the SLM and the recorded object. Therefore, in the process of hologram generation, the resolution of effective hologram is not 4K. As can be seen from Fig. 5, the wasted area of the hologram is filled to zero, then the final 4K hologram can be generated. Then the calculation speed of the proposed system can be improved greatly. When the resolution of the recorded object becomes larger, the difference will become more intuitive. At present, the calculation speed of hologram is relatively slow, so it is very necessary to improve the calculation speed. In the future research, it can be considered to make use of the wasted area of the SLM. For example, if an entire object can be diffracted from a wasted hologram area by using extra means, the viewing area of the reconstructed object will be further improved.

However, there are still some problems that need to be solved. For example, in the experiment, a BS is used to stitch the effective areas of two 2K SLMs. Then a Michelson interferometer can be created and the light diffracted by the two SLMs will interfere. To solve this problem, it is necessary to ensure that the reproduced light is completely collimated. In the experiment, the path difference between the two arms of the Michelson needs to be minimized. In addition, we can choose a more stable experimental platform to conduct experiments. The width of EVA is increased only in the horizontal direction by using the proposed system. In the next work, phase factor can be loaded on the edge section of the SLM to increase the EVA in the vertical direction. The resolution of the recorded object needs to be smaller than that of the 4K SLM. If the resolution of the recorded object is close to the 4K SLM, the quality of the reconstructed object will be decreased as the resolution of the effective hologram is too small. Therefore, the technology used in the proposed system is more advantageous for objects with a larger amount information within a certain range. This range is to ensure that the resolution of the recorded object is less than the resolution of the effective hologram. In this paper, two 2K SLMs are used to splice a 4K SLM. Currently, the 4K SLM is available on the market. Though the pixel size of the 4K SLM can reach 3.74 $\mu$m, the cost is very high. If two 4K SLMs are used for splicing, the perspective of the reconstructed object will be further improved. Today, seamless stitching based on multiple SLMs is an important way to expand the viewing angle

of the holographic display. If more SLMs are used in the proposed system, the viewing area will be further expanded than the traditional splicing method.

## 4. Conclusion

In this paper, a holographic display system is proposed based on the effective area expansion of the SLM. By calculating the effective area of the SLM based on the viewing area characteristics and seamlessly stitching the effective areas of two 2K SLMs, a 4K SLM is realized in the system. Then the effective area of the hologram is increased, and the calculation of wasted information is decreased compared with the traditional system. With the proposed system, the reconstructed object with large viewing area can be realized. Moreover, the calculation speed is improved. Experimental results verify the feasibility of the proposed system. In the proposed system, the 2K SLMs are used as examples for splicing. When more high-performance SLMs are used, the viewing area will be further expanded than the traditional splicing method. The proposed system can provide new ideas to the holographic display system based on multiple SLMs stitching.

## References

[1] Y. Wu *et al.*, "Design of retinal-projection and reflow process system," *Opt. Exp.*, vol. 26, no. 9, pp. 11553–11567, 2018.
[2] Z. Wang *et al.*, "Resolution-enhanced holographic stereogram based on integral imaging using moving array lenslet technique," *Appl. Phys. Lett.*, vol. 113, 2018, Art. no. 221109.
[3] M. L. Huebschman, B. Munjuluri, and H. R. Garner, "Dynamic holographic 3-D image projection," *Opt. Exp.*, vol. 11, no. 5, pp. 437–445, 2003.
[4] D. Wang, C. Liu, F. Chu, and Q. H. Wang, "Full color holographic display system based on intensity matching of reconstructed image," *Opt. Exp.*, vol. 27, no. 12, pp. 16599–16612, 2019.
[5] D. E. Smalley, Q. Y. J. Smithwick, V. M. Bove, J. Barabas, and S. Jolly, "Anisotropic leaky-mode modulator for holographic video displays," *Nature*, vol. 498, pp. 313–317, 2013.
[6] J. Park, K. Lee, and Y. Park, "Ultrathin wide-angle large-area digital 3D holographic display using a non-periodic photon sieve," *Nature Commun.*, vol. 10, p. 1304, 2019.
[7] D. Wang, C. Liu, and Q. H. Wang, "Holographic zoom micro-projection system based on three spatial light modulators," *Opt. Exp.*, vol. 27, no. 6, pp. 8048–8058, 2019.
[8] Y. Huang, E. Liao, R. Chen, and S. T. Wu, "Liquid-crystal on silicon for augmented reality displays," *Appl. Sci.*, vol. 8, no. 12, 2018, Art. no. 2366.
[9] H. M. P. Chen, J. P. Yang, H. T. Yen, Z. N. Hsu, Y. Huang, and S. T. Wu, "Pursuing high quality phase-only liquid crystal on silicon (LCoS) devices," *Appl. Sci.*, vol. 8, no. 11, 2019, Art. no. 2323.
[10] J. H. Park and S. B. Kim, "Optical see-through holographic near-eye-display with eyebox steering and depth of field control," *Opt. Exp.*, vol. 26, no. 21, pp. 27076–27088, 2018.
[11] T. Sugie *et al.*, "High-performance parallel computing for next-generation holographic imaging," *Nature Electron.*, vol. 1, pp. 254–259, 2018.
[12] Y. Takaki and N. Okada, "Hologram generation by horizontal scanning of a high-speed spatial light modulator," *Appl. Opt.*, vol. 48, no. 17, pp. 3255–3260, 2009.
[13] Y. Sando, D. Barada, and T. Yatagai, "Full-color holographic 3D display with horizontal full viewing zone by spatiotemporal-division multiplexing," *Appl. Opt.*, vol. 57, no. 26, pp. 7622–7626, 2018.
[14] Y. Matsumoto and Y. Takaki, "Time-multiplexed color image generation by viewing-zone scanning holographic display employing MEMS-SLM," *J. Soc. Inf. Display*, vol. 25, no. 8, pp. 515–523, 2017.
[15] M. Stanley *et al.*, "100 mega-pixel computer generated holographic images from active tiling TM—A dynamic and scalable electro-optic modulator system," *Proc. SPIE*, vol. 5005, pp. 247–258, 2003.
[16] Y. Takaki and J. Nakamura, "Zone plate method for electronic holographic display using resolution redistribution technique," *Opt. Exp.*, vol. 19, no. 15, pp. 14707–14719, 2011.
[17] J. Hahn, H. Kim, Y. Lim, G. Park, and B. Lee, "Wide viewing angle dynamic holographic stereogram with a curved array of spatial light modulators," *Opt. Exp.*, vol. 16, no. 16, pp. 12372–12386, 2008.
[18] T. Kozacki, M. Kujawinska, G. Finke, W. Zaperty, and B. Hennelly, "Holographic capture and display systems in circular configurations," *J. Disp. Technol.*, vol. 8, no. 4, pp. 225–232, 2012.
[19] N. Fukaya, K. Maeno, O. Nishikawa, and K. Matsumoto, "Expansion of the image size and viewing zone in holographic display using liquid crystal devices," *Proc. SPIE*, vol. 2406, pp. 283–289, 1995.
[20] F. Yaras, H. Kang, and L. Onural, "Multi-SLM holographic display system with planar configuration," in *Proc. IEEE 3DTV-Conf.*, 2010, pp. 1–4.
[21] F. Yaraş, H. Kang, and L. Onural, "Circular holographic video display system," *Opt. Exp.*, vol. 19, no. 10, pp. 9147–9156, 2011.
[22] D. D. Teng *et al.*, "Spatiotemporal multiplexing for holographic display with multiple planar aligned spatial-light-modulators," *Opt. Exp.*, vol. 22, no. 13, pp. 15791–15803, 2014.
[23] M. Agour, C. Falldorf, and R. B. Bergmann, "Holographic display system for dynamic synthesis of 3D light fields with increased space bandwidth product," *Opt. Exp.*, vol. 24, no. 13, pp. 14393–14405, 2016.

[24] Z. X. Zeng, H. D. Zheng, Y. J. Yu, A. K. Asundi, and S. Valyukh, "Full-color holographic display with increased-viewing-angle," *Appl. Opt.*, vol. 56, no. 13, pp. F112–F120, 2017.
[25] Y. Sando, K. Satoh, T. Kitagawa, M. Kawamura, D. Barada, and T. Yatagai, "Super-wide viewing-zone holographic 3D display using a convex parabolic mirror," *Sci. Rep.*, vol. 8, 2018, Art. no. 11333.
[26] X. Li, J. Liu, T. Zhao, and Y. Wang, "Color dynamic holographic display with wide viewing angle by improved complex amplitude modulation," *Opt. Exp.*, vol. 26, no. 3, pp. 2349–2358, 2018.
[27] E. Y. Chang *et al.*, "360-degree color hologram generation for real 3D objects," *Appl. Opt.*, vol. 57, no. 1, pp. A91–A100, 2018.
[28] M. Lucente, "Interactive computation of holograms using a look-up table," *J. Electron. Imag.*, vol. 2, no. 1, pp. 28–34, 1993.
[29] K. Yamamoto, Y. Ichihashi, T. Senoh, R. Oi, and T. Kurita, "Calculating the Fresnel diffraction of light from a shifted and tilted plane," *Opt. Exp.*, vol. 20, no. 12, pp. 12949–12958, 2012.
[30] T. Shimobaba, N. Masuda, and T. Ito, "Simple and fast calculation algorithm for computer-generated hologram with wavefront recording plane," *Opt. Lett.*, vol. 34, no. 20, pp. 3133–3135, 2009.
[31] S. C. Kim and E. S. Kim, "Fast one-step calculation of holographic videos of three-dimensional scenes by combined use of baseline and depth-compensating principal fringe patterns," *Opt. Exp.*, vol. 22, no. 19, pp. 22513–22527, 2014.
[32] S. Jiao, Z. Zhuang, and W. Zou, "Fast computer generated hologram calculation with a mini look-up table incorporated with radial symmetric interpolation," *Opt. Exp.*, vol. 25, no. 1, pp. 112–123, 2017.
[33] M. W. Kwon, S. C. Kim, S. E. Yoon, Y. S. Ho, and E. S. Kim, "Object tracking mask-based NLUT on GPUs for real-time generation of holographic videos of three-dimensional scenes," *Opt. Exp.*, vol. 23, no. 3, pp. 2101–2120, 2015.